

Analysing the Thought Process of EEG Pattern using Compressed Sensing Architecture

¹Arun Kumar S and ²Anand L

¹Department of Computer Science and Engineering,

¹School of Computing, SRM Institute of Science and Technology Potheri, Kattankulathur, Tamil Nadu, India.

²Department of Networking and Communications, School of Computing, SRM Institute of Science and Technology Potheri, Kattankulathur, Tamil Nadu, India.

¹aarunkumar889@gmail.com, ²anandl@srmist.edu.in

Correspondence should be addressed to Anand L: anandl@srmist.edu.in

Article Info

Journal of Machine and Computing (<https://anapub.co.ke/journals/jmc/jmc.html>)

Doi: <https://doi.org/10.53759/7669/jmc202505053>.

Received 10 May 2024; Revised from 26 August 2024; Accepted 22 December 2024.

Available online 05 April 2025.

©2025 The Authors. Published by AnaPub Publications.

This is an open access article under the CC BY-NC-ND license. (<https://creativecommons.org/licenses/by-nc-nd/4.0/>)

Abstract - Sleep pattern recognition plays a crucial role in detecting pathological and psychological diseases. Various disorders can be identified through analysis of EEG patterns recorded during sleep. Sleep EEG consists of four primary waveforms: alpha, beta, theta, and delta waves, each associated with different sleep stages. The cyclic alternating pattern (CAP) is characterized by cerebral activity and autonomic motor functions, providing insights into motor events and neurovegetative functions that aid in understanding the pathophysiology of sleep disorders. This research focuses on identifying sleep patterns using a Compressed Sensing Architecture (CSA). The aim is to assist pathologists in accurately and efficiently diagnosing sleep disorders through automated analysis. Existing methodologies for extracting sleep patterns from EEG rely on various algorithms. In this study, error signals are extracted using CSA, and metrics such as the Percentage Root-mean-square Difference (PRD) and Signal-to-Noise Ratio (SNR) are computed after reconstructing the original signal. The proposed approach demonstrates enhanced accuracy, making it a promising solution for automated, error-free diagnosis of sleep disorders. The research findings have significant potential for practical implementation, improving diagnostic precision and clinical outcomes.

Keywords – Brain Signal, SNR, Accuracy, PRD, Pre-Processing, Sleep Pattern.

I. INTRODUCTION

Sleep and Brain activities are closely connected, with technology like BCIs (Brain Computer Interfaces) utilizing these signals for advanced applications. Sleep is essential part of daily life during which the body and brain rest, consciousness and sensory activity reduce, clears the waste via Glymphatic system and the brain reorganizes the neurons. The Brain function improves when in sleep. The Brain activity during sleep is measured using EEG signals, which changes in amplitude and frequency depending on sleep stage. There are different frequencies and amplitudes for falling asleep, being asleep and being awake. Alpha waves appear during relaxation, Beta waves dominate during focus, Gamma waves during intense concentration, and Delta and Theta waves during deeper sleep. Analysing these patterns helps in diagnosing sleep disorders and understanding brain function.

BCIs takes brain signal analysis further by enabling humans to communicate with machines without speech or gestures. BCIs use sensors to collect brain activity data and translate it to commands for devices, often relying on EEG signals. EEG signals are sensitive to other bio-signals such as heart rate and eye movement, BCI incorporate additional inputs like electrocardiogram (ECG), photoplethysmography (PPG), electromyogram (EMG), electrooculogram (EOG), and Galvanic Skin Reflex (GSR) for greater accuracy. BCIs directly decode brain commands allowing control of devices like prosthetics or computer cursors, unlike traditional systems that rely on peripheral nerves. These bio-signals make it feasible to control external devices as well as computer applications. The technology is widely applied in fields such as healthcare, aerospace, education, entertainment and marketing and simplifying interactions with machines. These advancements and concerns about security and privacy remain as third-party misuse of personal data which is a significant risk. In the past, the idea that brain activity could be utilized to interpret thoughts or intentions was dismissed as unrealistic it was resulted as Research into brain activity was traditionally restricted to diagnosing neurological disorders or investigating brain activities. This limitation was due to the scarcity of information that could be reliably gathered from the human brain, making the design of a Brain-Computer Interface (BCI) seem prohibitively difficult. BCIs were once considered as

impractical due to limited technology and challenges of real-time signal processing but advancements in neuroscience, psychology, engineering and computer science have made BCIs more feasible. Researchers are now advocating a unified approach to BCI design to standardize developments and accelerate progress in the transformative field.

There are 5 Stages of sleep, the **Fig 1** shows different stages of sleep with respect to time. The sleepness and the wakefulness shows different stages in the Figure. Based on the specific type of sleep, the neural systems are being activated while the others being turned off. The neurobiology helps us to understand various stages of sleep. For many centuries, most of the people thought that the sleep is considered as a unitary phenomenon whose physiological he was essential. The purpose of sleep is just the restorative. In the 1953, Nathaniel Kleitman and Eugene Aserinsky Presented that. The sleep for actually comprises of different stages based on the electroencephalographic recordings. Whereas these stages occur sequentially, one after the other.

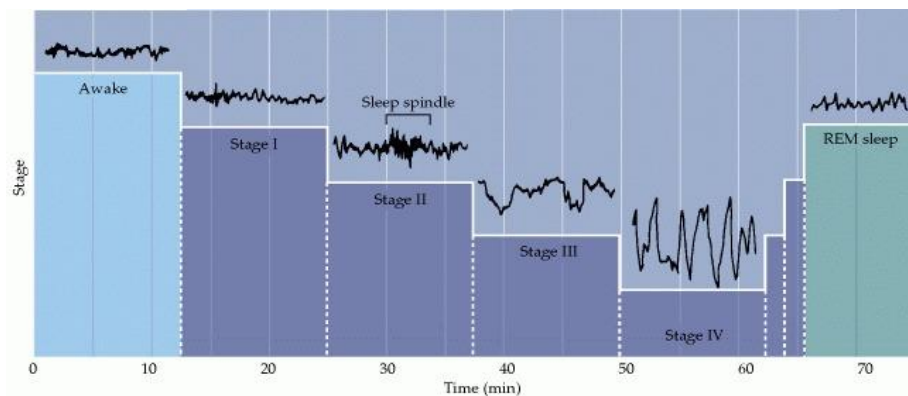


Fig 1. Stages of Sleep.

A high frequency of 50 to 60 Hz is recorded during the waking state after one hour of sleep. These signals have low amplitude (Approximately 30 microvolts) And they are fewer active signals. The **Fig 1**, shows one hour of EEG recording of first ever sleep. Patterns are called as beta activity.

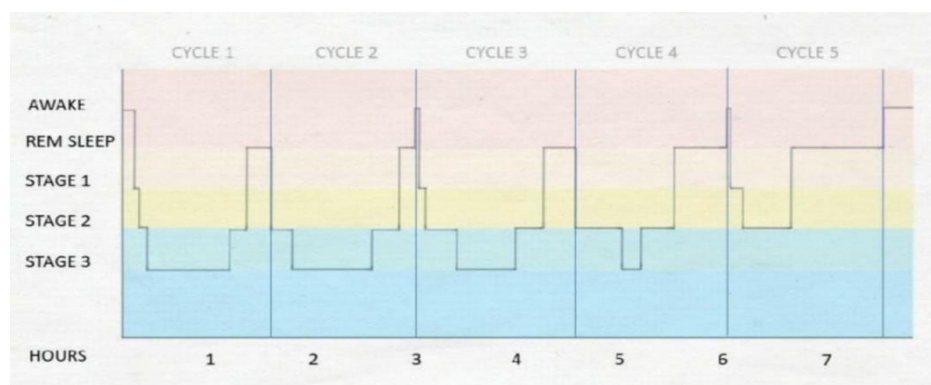


Fig 2. Sleep Cycles.

The sleep is classified into four stages (as in **Fig 2**) by American Academy of sleep medicine. Among the four sleep cycles, the first two stages are considered to be light sleep. When a person begins to fall asleep, he enters the Stage 1. During this, the EEG recorded will be having low amplitude waves with high frequency. When the person enters the Stage 2, The EEG signals will be having a sleep spindles and k-complexes (patterns in sleep EEG signals). A train of high frequency waves are called as a sleep spindles. The Biphasic waves that stand out from the rest of the EEG signal are called K complex. The slow wave sleep is the stage 3 of sleep. The third stage of the sleep is very important for the restfulness. Next, the sleeper passes rapidly back through stage two and stage one before entering rapid eye movement or REM sleep. In REM sleep stage of the EEG activity is very similar to the top of waking Stage or stage 1. Most of the vivid dreams occur in this Stage. Each cycle will last about 90 to 110 minutes in a normal human being. And it is repeated for about four to five times in a night, as shown in the **Fig 2** With the timeline.

Contribution and Motivation

The compressed sensing architecture (CSA) is employed to classify sleep patterns in EEG signals. In this research phase, the patterns have been analysed, and feature extraction has been completed. The CSA was used to extract error signals. Data were collected from 50 subjects with normal sleep. The error signals were extracted, and the original signals were reconstructed as detailed in earlier sections. The results demonstrate improved accuracy compared to existing systems and

highlight the potential of this method for practical applications, achieving results close to high accuracy. The experiment successfully extracted sleep patterns and facilitated automated detection of key parameters in EEG signals. As a continuation of this research, the approach can be extended to recognize paralyzed sleep patterns. The proposed method has shown effectiveness in accurately identifying patterns associated with paralyzed sleep.

Organization of the Paper

The first section of paper gives a brief introduction to the basic details of sleep and patterns in sleep. The importance of sleep and sleep disorders are mentioned. The existing system and the different methods used to extract the sleep pattern details are also mentioned in the second section literature review. The basics of the proposed algorithm with detailed explanation is given in the third section proposed algorithm. Results and discussion are the fourth section which gives the implementation results obtained for the experiment conducted, in this the detailed description of each waveform is mentioned. Last section is the conclusion and future scope which are the final part of the paper.

II. LITERATURE SURVEY

In [1], the Author explained the Most BCI games classified as serious games have primarily been designed with healthy individuals in mind. Since BCI aims to replace traditional Human-Computer Interaction (HCI) in this context, it must effectively of Recent advancements in interpreting brain activity have enabled the conversion of neural signals into meaningful commands, facilitating applications such as smooth gameplay. With the availability of consumer-grade EEG equipment, the first BCI-controlled games were developed. These games can be categorized as either competitive entertainment games or medically focused serious games [2]. In [3],[4] The Authors analysed the BCI-controlled home automation system can manage various household components, including light fixtures, switches, and ceiling fans.

The combination of EEG, Variational Mode Decomposition (VMD), Support Vector Machine (SVM), and Predictor Importance Estimate (PIE) achieved remarkable performance metrics for diagnosing autism spectrum disorder (ASD), including an accuracy of 98.08%, sensitivity of 100%, specificity of 99.16%, precision of 99.17%, F1-score of 99.58%, and a geometric mean of 99.57% [5]. In [6] Using EEG data, the combination of Independent Component Analysis (ICA), Power Spectrum Density Energy Diagram (PSDED), and a Deep Convolutional Neural Network (DCNN) achieved an accuracy of 80% for classifying Autism and Epilepsy. The combination of EOG and EEG signals processed with a Bandpass Filter, Filter Bank Common Spatial Pattern (FBCSP), and Support Vector Machine (SVM) achieved an accuracy of 87.31% in the application of vehicle control [7]. Electroencephalography (EEG) signals processed using a filter, statistical analysis, and Principal Component Analysis (PCA) with a Long Short-Term Memory (LSTM) network achieved an accuracy of 82.4% for hand gesture decoding [8]. In [9] Magnetoencephalography (MEG) signals processed with a low-pass Butterworth filter, a notch filter, an autoencoder, and a Support Vector Machine (SVM) achieved an accuracy of 82.08% for neural speech decoding.

EEG signals processed for artifact removal using RNN, CNN, and XGBoost achieved an accuracy of 95.53% in the application of typing [10]. EEG signals processed with low-pass, high-pass, and notch filters alongside a CNN achieved an accuracy of 55.33%, a standard deviation of 3.615%, and a kappa value of 0.173 in the application of object movement [11]. Functional near-infrared spectroscopy (fNIR) signals processed with a high-pass filter combined with a Deep Neural Network (DNN) has achieved remarkable accuracy of 66% in various applications [12]. EEG signals processed with a bandpass filter, Fast Fourier Transform (FFT), and on-line for instance, the Online Sequential Extreme Learning Machine (OS-ELM) achieved an accuracy of 97.62%, a sensitivity of 97.55%, and a specificity of 99% in wheelchair control applications [13]. The time series data can be effectively analysed by extracting features from the detailed coefficients at different levels of resolution or within specific frequency bands, depending on the context.

Classification Methods

In BCI systems, various classification algorithms are employed [14][15]. Over-sampling can be employed to create an over-complete lexicon from a complete dictionary by sampling from it. While the dictionary's basis is orthogonal, this orthogonality may no longer hold after oversampling. Through iterative cycles, the Signal Decomposition Matrix (SDM) of the signal is constructed. Each iteration selects the optimal waveform based on the highest inner product between it and the residual signal.

Feature Extraction

The extracted features are then fed into a classifier for training, which helps recognize patterns. However, due to technical and biological factors—such as the subject's attention, session variability, mental state, anatomical differences, amplifier quality, and ambient noise—EEG signals are highly nonstationary and dynamic [16]. Galvanic Skin Response (GSR) [17] as a complement to EEG in BCI. Electromyography (EMG) [18].

Database

The database includes recordings from 16 healthy subjects with no neurological issues and not using any CNS-affecting drugs. The remaining 92 recordings come from patients where EEG technology is being used to diagnose and study various sleep disorders, including Nocturnal Frontal Lobe Epilepsy (NLE), Rapid Eye Movement Sleep Behaviour Disorder

(RBD), Periodic Limb Movement Disorder (PLM), insomnia, narcolepsy, Sleep-Disordered Breathing (SDB), and bruxism. Demographic information such as age and gender are available in a spreadsheet named "gender-age.xlsx," and the recordings are labelled according to the subject's sleep disorder. The instability of sleep is referred to as CAP (Cycling Alternating Pattern). CAP typically occurs during non-rapid eye movement (NREM) sleep and is divided into two phases: A and B. Phase A is characterized by irregularity, allowing for adaptive adjustments to ongoing states based on internal and external inputs. In contrast, phase B is considered the background rhythm of CAP. CAP involves both cerebral activity and autonomic motor functions. Several sleep disorders can be identified through the analysis of CAP, as it reflects motor events and neurovegetative functions, aiding in the understanding of physiological pathways in sleep disturbances.

The experimental data for sleep patterns in EEG signals is sourced from PhysioNet. The focus is on Cyclic Alternating Patterns (CAP), which reflect the brain's instability during sleep. CAP, characterized by periodic abnormal brain activity, is a marker of unstable sleep and does not occur during REM sleep. In conditions like Lennox-Gastaut syndrome, CAP helps control seizures and epileptic discharges through a gate-control mechanism. This section introduces the Compressed Sensing architecture. The first part provides an overview of the architecture, while the second part discusses the dynamic knob in compressed sensing. The third part formulates the actual problem.

The Sleep disruptions can interfere with neural functions, and in-ear electroencephalography (EEG) is employed to collect EEG signals from patients, providing a 24/7 unobtrusive monitoring method. The experiment involved 22 healthy participants undergoing overnight sleep monitoring. This method aims to predict automatic sleep stages using ear-EEG from a single in-ear sensor. The overall classification accuracy of the five sleep stages, calculated using PSG, was 74.1%. The ear sensor proved to be a feasible tool for monitoring overnight sleep, aligning with the PSG. This continuous, wearable alternative offers a convenient option for analysing sleep data around the clock.

III. PROPOSED ALGORITHM

The implementation process consists of multiple stages, each involving algorithms that analyze sleep patterns in EEG signals. The first stage in the front-end analysis employs a technique called Adaptive Quantized Compressive Sensing. This approach is an advanced method that integrates the principles of quantized compression sensing with adaptive mechanisms, allowing for efficient data representation and improved analysis of EEG signals.

Adaptive quantized compress sensing

This technique is a relatively new approach for converting analog signals into an information sampling scheme. It is designed to work efficiently under the assumption that the signal is sparse or compressible, meaning that it contains a limited number of significant components compared to its overall size. In this scheme, an N -dimensional vector is sampled using M measurements to produce a compressed representation of the vector a . These measurements satisfy certain fundamental conditions to ensure accurate reconstruction and effective data analysis.

$$a = \Phi b \quad (1)$$

In the equation (1), the $\Phi \in \mathbb{Q}^{m \times n}$, is called the sensing array with the linear encoding. The sampling rate is defined by M in the N Compressed sensing. In this context, the sensing matrix Φ is typically modeled as either a Bernoulli Random Variable or a Gaussian Random Variable, depending on the specific application. A key condition for the system is that the number of measurements M is much smaller than the signal dimension N (i.e., $M \ll N$), as outlined in Equation (1). Under these conditions, the signal cannot be uniquely retrieved directly from the sensing array. However, by leveraging certain sparsity constraints, it becomes possible to recover the signal accurately. Specifically, the sparsity condition allows the inclusion of a transform matrix $\Psi \in \mathbb{Q}^{N \times N}$, which represents the signal in terms of a set of sparse coefficients $c \in \mathbb{Q}^N$. This transformation enables the signal to be reconstructed effectively, even with limited measurements, by exploiting the sparse nature of the coefficients.

$$b = \Psi c \quad (2)$$

In the above equation (2), the under transformations Ψ , is having the count of zero elements. So, considering the equations (1) and (2), the spars vector is represented as below equation (3).

$$a = \Phi \Psi c = \Theta M \times N c \quad (3)$$

In Equation (3), the matrix $\Theta_{M \times N}$ is referred to as the measurement matrix, which plays a critical role in signal acquisition. In practical applications, the original form of any signal is typically analog. Before the signal can be processed or transmitted digitally, it must undergo a quantization process. Quantization is essential for converting the continuous analog signal into a discrete digital form suitable for further analysis. Once quantized, the next step is to compress the resulting signal a . This compression is achieved using a quantization model, which is mathematically represented in Equation (4). This process ensures efficient storage and transmission while preserving essential information from the original signal.

$$\hat{a} = R_x(a) \quad (4)$$

In the above equation R_x , is called the quantization Function. \hat{a} is the representation of the a with the quantization bits x . As we know the c is a sparse vector. Hence

$$\hat{c} = \min \|c\|_0 \quad \text{subject to } \|\hat{a} - \Theta c\| < \epsilon \quad (5)$$

The reconstruction error margin is denoted by ϵ , which defines the permissible deviation in the signal reconstruction process. Equation (5) provides a unique solution for the reconstruction, ensuring that the recovered signal adheres to the defined error constraints. One common approach to solving Equation (5) involves approximating the solution by reformulating the problem into an optimization task. This is achieved by minimizing a specific formulation, transitioning the problem into a structured minimization framework that simplifies computation while maintaining accuracy.

$$\hat{c} = \min \|c\|_1 \quad \text{subject to } \|\hat{a} - \Theta c\| < \epsilon \quad (6)$$

The ℓ_1 -minimization approach is a convex optimization problem, which makes it computationally efficient and solvable within polynomial time. This property is particularly advantageous for practical applications where quick and reliable solutions are required. As a result, the reconstructed signal \hat{b} can be accurately represented using this method. This approach ensures both efficiency and precision in signal reconstruction tasks.

$$\hat{a} = \psi \hat{c} \quad (7)$$

Adaptive Compressed Sensing Architecture

This section introduces the proposed Compressed Sensing architecture, outlining its key components and functionality. The first part provides an overview of the architecture, offering insights into its structure and purpose. The second part delves into the concept of a dynamic knob, which plays a crucial role in optimizing the compressed sensing process. Finally, the third part focuses on formulating the core problem, laying the foundation for the subsequent analysis and solution strategies.

Architecture Overview

The proposed adaptive compressed sensing architecture is designed to enhance EEG-based analysis of sleep patterns. This algorithm features dynamic reconfiguration, allowing it to adjust its components in response to the input signals provided through the EEG. The architecture, as depicted in **Fig 3**, consists of four key components: the dynamic web module, which manages real-time adjustments; the randomized encoding module, responsible for efficiently encoding the signals; the quantization module, which converts the continuous EEG signals into discrete values; and the signal reconstruction module, which reconstructs the signal for further analysis. Together, these components work synergistically to improve the accuracy and efficiency of sleep pattern detections

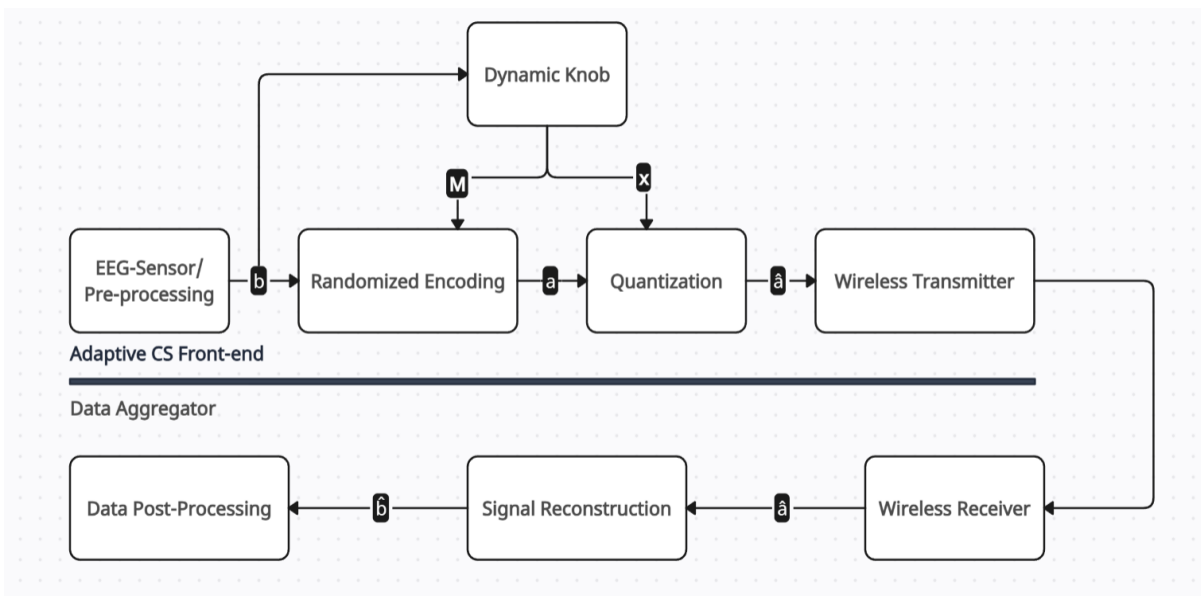


Fig 3. The Block Diagram Representation of Compressed Sensing Architecture.

Sensors collect analog inputs, also known as raw analog data $c \in \mathbb{Q}^N$. These signals are analyzed by a system called the dynamic knob, which examines the structure of the signals. The dynamic knob then adjusts the system's settings using an

optimal parameter estimator to ensure the best performance. It carries out two key tasks: converting the signals into digital form (quantization) and encoding them in a randomized way for efficient processing (randomized encoding).

In This System, The Analog Data B Is Encoded into an M -Dimensional Vector

$a \in Q^M$ using an encoding matrix $\Theta_{M \times N}$. Each bit is processed through a quantization scheme R_x , and the resulting digital data is represented as \hat{a} . The data aggregator collects this encoded information from a wireless transmitter.

Within the aggregator, a reconstruction algorithm is implemented to recover the original N -dimensional input signal b . At the heart of the Adaptive Compressed Sensing (ACS) architecture is the Dynamic Knob. This component acts like the central nervous system, managing and coordinating the activities of all modules. It ensures that the system adapts to the EEG signals and optimally configures the other modules for accurate signal processing.

To evaluate the CSA in terms of energy and the performance, the ACS model for energy is mentioned as below.

$$E = J \times M \times I \quad (8)$$

In Equation (8), M represents the sampling rate, I denote the bit resolution and refers J to the energy per bit in wireless communication. The Percentage Root Mean Square Difference (PRD) is defined in Equation (9).

$$PRD = \frac{\|b - \hat{b}\|_2}{\|b\|_2} \times 100\% \quad (9)$$

Percentage Root-Mean-Square Difference (PRD), which is often used to quantify the difference between an original signal (b) and its reconstructed or approximated version (\hat{b}), $\|b - \hat{b}\|_2$ - represents the Euclidean norm (or L_2 -norm) of the difference between the original signal (b) and the reconstructed signal (\hat{b}). $\|b\|_2$ - is the L_2 -norm (Euclidean norm) of the original signal b , essentially measuring the magnitude of b and $\times 100\%$ - Multiplying by 100 converts the result into a percentage for easier interpretation.

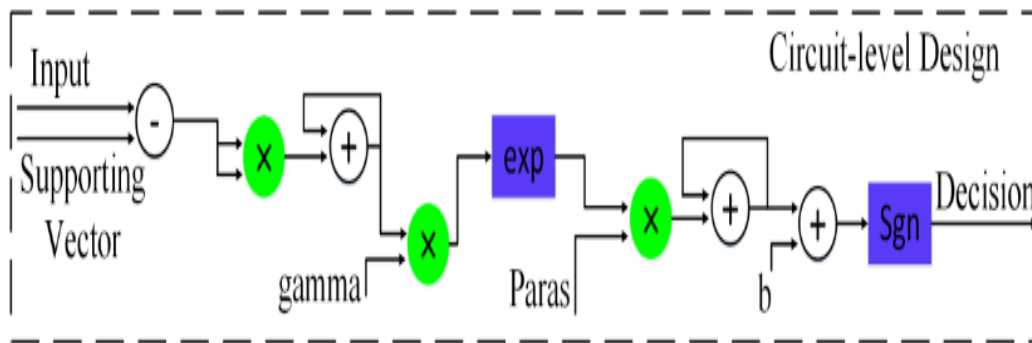


Fig 4. The Dynamic Knob Structure.

To achieve high accuracy and low-power design in EEG signal processing, the Dynamic Knob Framework plays a critical role in the design architecture. This framework ensures the mobility of the front-end EEG signals while maintaining efficient performance. It consists of two key components:

- Signal Structure Analyzer
- Configuration Lookup Table

The Configurable Pre-Calculator manages adjustable parameters, and ultra-low-power memory technology is employed to configure this structure. The primary goal is to create a highly accurate and energy-efficient signal structure within the analyzer. The basic block structure of the Dynamic Knob is depicted in **Fig 4**.

The Support Vector Machine (SVM) scheme is integrated into the Signal Structure Analyzer. The initial step involves a binary SVM classifier, which focuses on two critical factors: energy efficiency and classification accuracy. Accuracy is improved using a robust training dataset, while energy consumption is optimized through circuit-level implementation of the binary SVM classifier. The key challenge addressed by the Dynamic Knob Framework is solving the problem of multi-class classification.

In the first-level implementation of the binary SVM classifier, handling the multi-class classification problem becomes a top priority. The Radial Basis Function (RBF) and Time-Division Multiplexing (TDM) kernel are utilized for classification tasks, with the CORDIC Algorithm enabling efficient SVM implementation.

The algorithm calculates differences between input vectors to generate support vectors. Multipliers are used for squaring operations, and the sum of all squared values is combined to form specific parameters. These parameters, determined using the CORDIC algorithm, are crucial for computing exponentials and other elements in Equation (10). This approach enhances both classification performance and energy efficiency in the Dynamic Knob Framework.

$$\text{parasi} = a_i \times \alpha \quad (10)$$

The authors have proposed an automatic sleep spindle detection system, working with EEG signals from background activity. The system combines two approaches. The first approach filters the EEG signal to isolate Sigma band frequencies, while the second approach imitates the procedure of expert analysis. Sleep spindle detection is only considered valid when both approaches produce consistent results. The testing included EEG recordings from two subjects; thus, an aggregate number of 1,132 epochs was achieved. Sleep spindle events were identified for 803 instances by experts and the developed model achieved accuracy of 87.7%. The study of sleep spindles has various applications for humans, such as the detection of nervous system diseases, nutritional deficiencies, and risk assessment for diseases including sudden infant death syndrome. A polymorphic graph is used to analyse sleep patterns among adults and children.

The detected virtual patterns are considerable for psychological and pathological studies. Five characteristic patterns for sleep are identified in the paper: slow delta and theta waves, EEG activity spindles, rapid eye movement (REM) sleep, and EMG muscle tone. EEG samples are collected at 250 Hz, and two discrimination approaches are processed in parallel, classified as Module 1 and Module 2. In Module 1, the Sigma band filter is applied, while Module 2 utilizes a mimicking approach. Both modules filter and analyse the ECG signal in the time domain, and analysis is conducted based on different criteria. The findings are condensed in Module 3 and set up the acceptable parameters in relation to the requirements of the system specifications. Several parameters are used in fine-tuning and training of the data to establish a correct threshold for the signals.

Throughout the study, anterior derivations were studied, using direct references for both background activity and anterior activation. The system was tested on continuous sleep recordings from a pair of patients, amounting to a total of 1,132 epochs. Experts identified 803 occurrences of sleep spindle events, and the results were tabulated, showing an average accuracy of prediction at 87.7%. Sleep is an integral part of human life and is associated with distinct brain wave patterns, which is actually a state of both physical and mental rest. The fundamental feature of sleep is changed consciousness, which is usually associated with reduced sensory perception, muscular activity, and environmental interaction. During the course of sleep, brain activity is increased, and neural circuits are remodelled. In addition, central nervous system promotes the brain Glymphatic system space clearance. These amplitude and frequency variations of the sleep cycle are observable in the EEG signals as the variations that correspond to the states - falling asleep, asleep, or awake. Various stages present different brain waves, Alpha waves typically occur when a person is resting. Other brain waves include Beta, Theta, Gamma, and Delta waves, each associated with different states of brain activity. Beta waves are observed when an individual focus on a particular aspect. This is a function of high frequencies and less amplitude. Gamma waves are used when a person is greatly engaged in an activity. These include Delta and Theta waves in the deeper stages of sleeping.

IV. RESULTS AND DISCUSSION

Parameters of Analysis

This experimental result analyses are done two key parameters: Signal-to-Noise Ratio (SNR) and Percentage Root Mean Square Difference (PRD). In simple terms, SNR refers to the ratio between the desired information signal and the undesired background noise, indicating the signal's clarity. PRD, which stands for Percentage Root Mean Square Difference, is a quality metric used to evaluate the accuracy of EEG signal reconstruction after compression. It reflects the improvement in signal reconstruction, with lower PRD values indicating better quality.

The research experiment was conducted on 50 patients, with their sleep patterns recorded as EEG signals. The signals were pre-processed, and the error signals were extracted as illustrated in **Fig 5** to 10. A sample from two subjects is presented below.

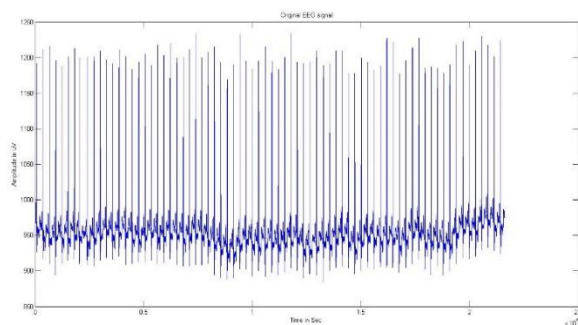


Fig 5. The Original EEG Signals of Sample Subject 1.

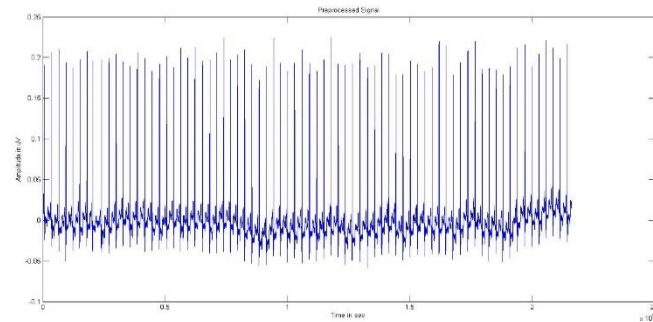


Fig 6. The Pre-Processed EEG Signals of Sample Subject 1.

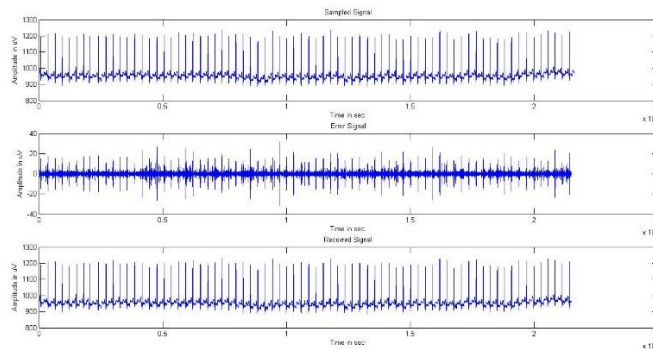


Fig 7. The Recovered Signal Obtained After the Reconstruction for the EEG Signals Taken Form Sample Subject -1.

The **Fig 5** shows the original EEG signals that are taken from the patient 1(subject 1). The signals are loaded in to the MATLAB code to perform the pre-processing by feature extraction, these results are shown in the **Fig 6**. The error signals ate extracted, and the original signals are reconstructed form the it. This is shown in **Fig 7**. The above results are the taken for the sampling value $N = 32$. The same has been carried out for $N=32,64,128,256,512,1024$.

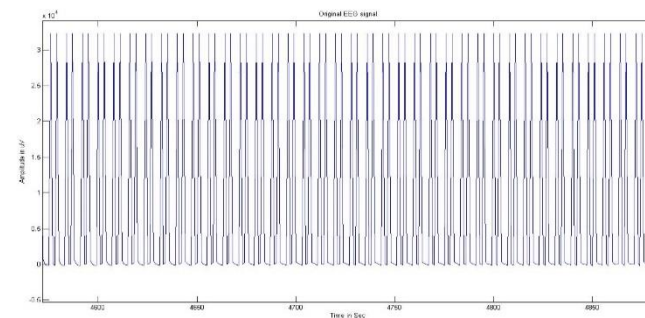


Fig 8. The Original EEG Signals of Sample Subject 2.

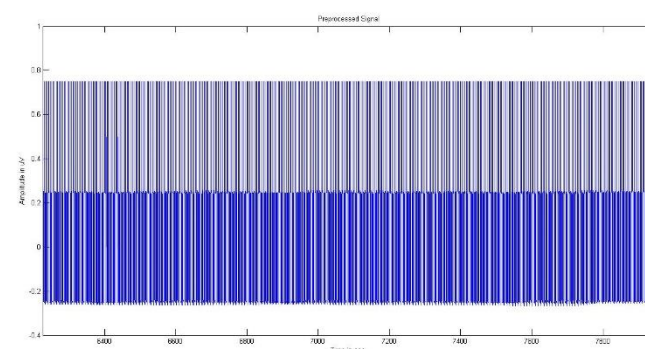


Fig 9. The Pre-Processed EEG Signals of Sample Subject 2.

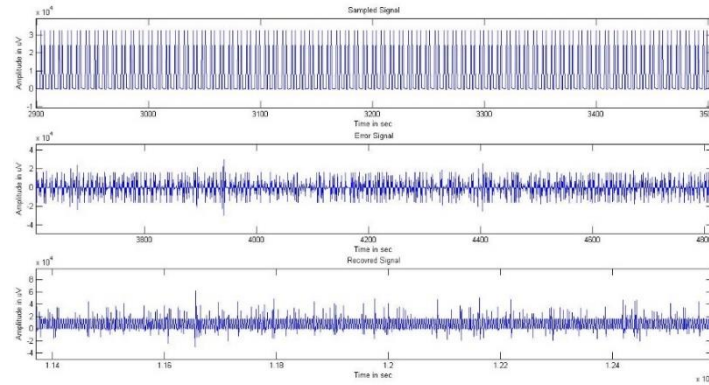


Fig 10. The Recovered Signal Obtained After the Reconstruction for The EEG Signals Taken Form Sample Subject -2.

The **Fig 8**, shows the original EEG signals that are taken from the patient 1(subject 1). The signals are loaded in to the MATLAB code to perform the pre-processing by feature extraction, these results are shown in the **Fig 9**. The error signals are extracted, and the original signals are reconstructed form the it. This is shown in **Fig 10**. The above results are the taken for the sampling value $N = 32$. The same has been carried out for $N=32,64,128,256,512,1024$.

Table 1. PRD And SNR Values for Different Samples

Samples	PRD	SNR	Samples	PRD	SNR	Samples	PRD	SNR
1	0.77383	82.2271	18	0.773	82.396	35	0.7712	82.3967
2	0.74635	82.5412	19	0.764	82.4559	36	0.761	82.4779
3	0.74763	82.5263	20	0.761	82.389	37	0.759	82.3284
4	0.78882	82.0605	21	0.7681	82.536	38	0.7528	82.398
5	0.7666	82.3086	22	0.7554	82.3209	39	0.7693	82.4712
6	0.78056	82.223	23	0.7704	82.2252	40	0.7759	82.432
7	0.7752	82.3283	24	0.7583	82.261	41	0.7701	82.5159
8	0.765	82.4847	25	0.7609	82.3145	42	0.7557	82.4693
9	0.7531	82.2686	26	0.756	82.5072	43	0.7718	82.474
10	0.7885	82.3477	27	0.7563	82.3264	44	0.7522	82.4662
11	0.7773	82.3703	28	0.7807	82.3483	45	0.7824	82.4528
12	0.7879	82.424	29	0.7845	82.5299	46	0.7632	82.5444
13	0.7503	82.4273	30	0.7625	82.4763	47	0.7646	82.5188
14	0.7744	82.5102	31	0.7858	82.4582	48	0.7735	82.2928
15	0.77	82.4081	32	0.7816	82.2757	49	0.7716	82.2777
16	0.7628	82.3879	33	0.7757	82.3036	50	0.752	82.2349
17	0.7701	82.2671	34	0.7566	82.2618			

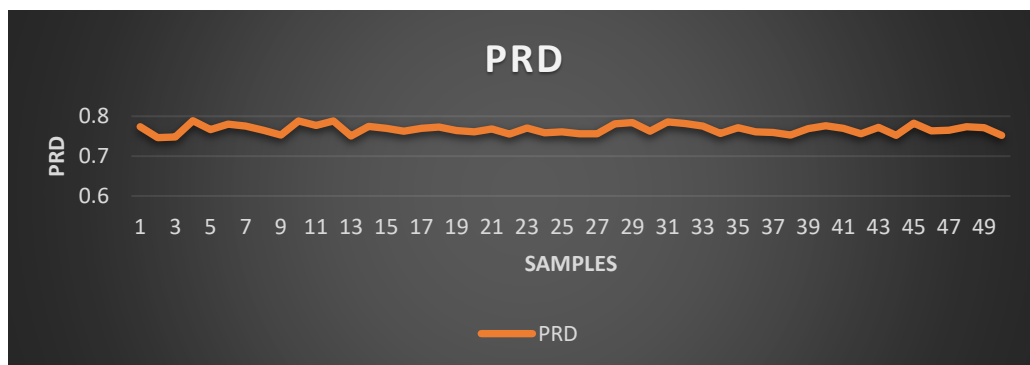


Fig 11. The Computed PRD Values For 50 Sample Subjects.

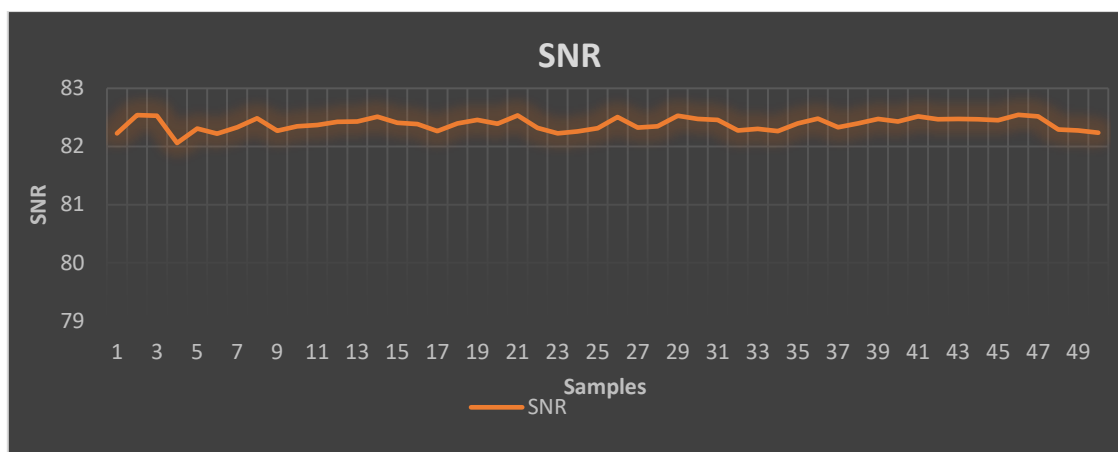


Fig 12. The Computed SNR Values For 50 Sample Subjects.

The **Table 1** is the consolidated values of the PRD and SNR values for the different samples. **Fig 11** and **Fig 12** are the plots of the same table. The values of SNR and PRD shows consistency with respect to different samples.

V. CONCLUSION AND FUTURE WORK

The compressed sensing architecture (CSA) is utilized to classify sleep patterns in EEG signals. At this stage of the research, the patterns have been analyzed, and feature extraction has been performed. The error signal is extracted using the CSA. Data were collected from 50 subjects with normal sleep. For all subjects, the PRD (Percentage Root Difference) and SNR (Signal-to-Noise Ratio) were calculated, with the results tabulated in **Table 1** and plotted in **Figs 11** and **12**. The mean PRD and SNR values were determined to be 82.38496 dB and 0.76751 dB, respectively, averaged across a sampling range of $N=32$ to $N=1024$. The error signals were extracted, and the original signals reconstructed, as detailed in the preceding sections. The obtained results demonstrate improved accuracy compared to existing systems. This method shows potential for practical applications, as the results are close to achieving high accuracy. The experiment successfully extracted sleep patterns and enabled automated detection of relevant parameters in EEG signals. As a continuation of this research, the method can be extended to include the recognition of paralyzed sleep patterns. This approach has proven effective in accurately identifying patterns associated with paralyzed sleep.

CRedit Author Statement

The authors confirm contribution to the paper as follows:

Conceptualization: Arun Kumar S and Anand L; **Methodology:** Arun Kumar S; **Software:** Arun Kumar S and Anand L; **Data Curation:** Anand L; **Writing- Original Draft Preparation:** Arun Kumar S and Anand L; **Visualization:** Arun Kumar S; **Investigation:** Anand L; **Supervision:** Arun Kumar S and Anand L; **Validation:** Arun Kumar S; **Writing-Reviewing and Editing:** Arun Kumar S and Anand L; All authors reviewed the results and approved the final version of the manuscript.

Data Availability

No data was used to support this study.

Conflicts of Interests

The author(s) declare(s) that they have no conflicts of interest.

Funding

No funding agency is associated with this research.

Competing Interests

There are no competing interests

References

- [1]. G. Cattani, "The Use of Brain-Computer Interfaces in Games Is Not Ready for the General Public," *Frontiers in Computer Science*, vol. 3, Mar. 2021, doi: 10.3389/fcomp.2021.628773.
- [2]. C. Gezeze and E. Kacar, "Virtual Character Control by Brain-Computer Interface and Comparison of Performance Metrics," 2021 International Conference on INnovations in Intelligent SysTems and Applications (INISTA), pp. 1–7, Aug. 2021, doi: 10.1109/inista52262.2021.9548604.
- [3]. T. Roopa Rechal, P. Rajesh Kumar, and Sk. Ebraheem Khaleelulla, "A Feasibility Approach in Diagnosing ASD with PIE via Machine Learning Classification Approach using BCI," 2021 International Conference on Computing, Communication, and Intelligent Systems (ICCCIS), pp. 557–562, Feb. 2021, doi: 10.1109/icccis51004.2021.9397220.

- [4]. M. Ranjani and P. Supraja, “Classifying the Autism and Epilepsy Disorder Based on EEG Signal Using Deep Convolutional Neural Network (DCNN),” 2021 International Conference on Advance Computing and Innovative Technologies in Engineering (ICACITE), pp. 880–886, Mar. 2021, doi: 10.1109/icacite51222.2021.9404634.
- [5]. S. D. T. Olesen, R. Das, M. D. Olsson, M. A. Khan, and S. Puthusserypady, “Hybrid EEG-EOG-based BCI system for Vehicle Control,” 2021 9th International Winter Conference on Brain-Computer Interface (BCI), pp. 1–6, Feb. 2021, doi: 10.1109/bci51272.2021.9385300.
- [6]. J. Pradeepkumar, M. Anandakumar, V. Kugathasan, T. D. Lalitharatne, A. C. De Silva, and S. L. Kappel, “Decoding of Hand Gestures from Electrooculography with LSTM Based Deep Neural Network,” 2021 43rd Annual International Conference of the IEEE Engineering in Medicine & Biology Society (EMBC), pp. 420–423, Nov. 2021, doi: 10.1109/embc46164.2021.9630958.
- [7]. D. Dash, A. Wisler, P. Ferrari, E. M. Davenport, J. Maldjian, and J. Wang, “MEG Sensor Selection for Neural Speech Decoding,” IEEE Access, vol. 8, pp. 182320–182337, 2020, doi: 10.1109/access.2020.3028831.
- [8]. X. Zhang, L. Yao, Q. Z. Sheng, S. S. Kanhere, T. Gu, and D. Zhang, “Converting Your Thoughts to Texts: Enabling Brain Typing via Deep Feature Learning of EEG Signals,” 2018 IEEE International Conference on Pervasive Computing and Communications (PerCom), pp. 1–10, Mar. 2018, doi: 10.1109/percom.2018.8444575.
- [9]. E. Petoku and G. Capi, “Object Movement Motor Imagery for EEG based BCI System using Convolutional Neural Networks,” 2021 9th International Winter Conference on Brain-Computer Interface (BCI), pp. 1–5, Feb. 2021, doi: 10.1109/bci51272.2021.9385319.
- [10]. G. Huve, K. Takahashi, and M. Hashimoto, “Brain-computer interface using deep neural network and its application to mobile robot control,” 2018 IEEE 15th International Workshop on Advanced Motion Control (AMC), pp. 169–174, Mar. 2018, doi: 10.1109/amc.2018.8371082.
- [11]. M. F. Ansari, D. R. Edla, S. Dodia, and V. Kuppili, “Brain-Computer Interface for wheelchair control operations: An approach based on Fast Fourier Transform and On-Line Sequential Extreme Learning Machine,” Clinical Epidemiology and Global Health, vol. 7, no. 3, pp. 274–278, Sep. 2019, doi: 10.1016/j.cegh.2018.10.007.
- [12]. N. Thillaiarasu, S. Lata Tripathi, and V. Dhinakaran, Artificial Intelligence for Internet of Things. CRC Press, 2022. doi: 10.1201/9781003335801.
- [13]. A. Bablani, D. R. Edla, D. Tripathi, and R. Cheruku, “Survey on Brain-Computer Interface,” ACM Computing Surveys, vol. 52, no. 1, pp. 1–32, Feb. 2019, doi: 10.1145/3297713.
- [14]. M. Bueno-Lopez, P. A. Munoz-Gutierrez, E. Giraldo and M. Molinas, “Electroencephalographic Source Localization based on Enhanced Empirical Mode Decomposition,” IAENG International Journal of Computer Science, Vol. 46, No. 2, pp. 228–236, (2019).
- [15]. N. F. Ozkan and E. Kahya, “Classification of BCI Users Based on Cognition,” Computational Intelligence and Neuroscience, vol. 2018, pp. 1–10, 2018, doi: 10.1155/2018/6315187.
- [16]. A. Chowdhury, H. Raza, Y. K. Meena, A. Dutta, and G. Prasad, “An EEG-EMG correlation-based brain-computer interface for hand orthosis supported neuro-rehabilitation,” Journal of Neuroscience Methods, vol. 312, pp. 1–11, Jan. 2019, doi: 10.1016/j.jneumeth.2018.11.010.
- [17]. M. C. Massi and F. Ieva, “Learning Signal Representations for EEG Cross-Subject Channel Selection and Trial Classification,” 2021 IEEE 31st International Workshop on Machine Learning for Signal Processing (MLSP), pp. 1–6, Oct. 2021, doi: 10.1109/mlsp52302.2021.9596522.
- [18]. J. Onners, M. Alam, B. Cichy, N. Wymbs, and J. Lukos, “U-EEG: A Deep Learning Autoencoder for the Detection of Ocular Artifact in EEG Signal,” 2021 IEEE Signal Processing in Medicine and Biology Symposium (SPMB), pp. 1–5, Dec. 2021, doi: 10.1109/spmb52430.2021.9672271.